EARTHQUAKE ENGINEERING AND STRUCTURAL DYNAMICS, VOL. 25, 483–496 (1996)

ENERGY INPUT AND DISSIPATION BEHAVIOUR OF STRUCTURES WITH HYSTERETIC DAMPERS

MASAYOSHI NAKASHIMA*
Disaster Prevention Research Institute, Kyoto University, Gokasho, Uji, Kyoto 611, Japan

KAZUHIRO SABURI†
Building Design Department, Osaka Main Office, Takenaka Co. Ltd., 2-3-10, Nishi-honmachi, Nishi, Osaka 550, Japan

AND

BUNZO TSUJI‡
Department of Construction Engineering, Kobe University, Rokkodai, Nada, Kobe, 657, Japan

SUMMARY

This paper presents qualitative investigations on the energy behaviour of structures into which hysteretic dampers are incorporated. Emphasis was given to the ratio of the structural stiffness after the yielding of hysteretic dampers to the initial elastic stiffness, with a premise that this ratio, termed α in this study, tends to be large for structures with hysteretic dampers. Structures concerned were represented by discrete spring–mass systems having bilinear restoring force behaviour, in which the second stiffness relative to the initial stiffness is α. It was found that with the increase of α the total input energy tends to increase, but the increase is confined to a narrow range of natural periods. Both the total input energy and hysteretic energy were found to become less sensitive to the yield strength with the increase of α. A simple formula was also proposed to estimate the maximum deformation given the knowledge of the hysteretic energy. Analysis of MDOF systems revealed that, even when α is large, the total input energy and hysteretic energy for MDOF systems are approximately the same as those of the equivalent SDOF system, and the hysteretic energy can be distributed uniformly over the stories if α is large.

KEY WORDS: hysteretic damper; input energy; hysteretic energy; seismic design; distribution of damage

INTRODUCTION

The backbone of the study presented herein consists of (1) development of structural systems having hysteretic dampers and (2) introduction of energy-based seismic design. In recent years, research has been flourishing on the development of various damping mechanisms that are incorporated into structures in order to achieve positive control of structural vibrations induced by wind and earthquakes. Popular among these new mechanisms are friction dampers, viscous dampers, viscoelastic dampers, and hysteretic dampers, all of which are passive damping mechanisms. Details of these dampers and their applications have been presented in numerous papers, and reports on their state of the art have also been made available, for example, in References 1 and 2 among many others. In this paper, special attention is paid to hysteretic dampers that, for energy dissipation, rely on the hysteresis of their materials, such as structural steels. A few examples of hysteretic dampers are: steel-plate added damping and stiffness devices,[3] referred to as ADAS

* Associate Professor
† Engineer
‡ Professor

CCC 0098–8847/96/050483–14

Received 22 November 1994
Revised 30 November 1995

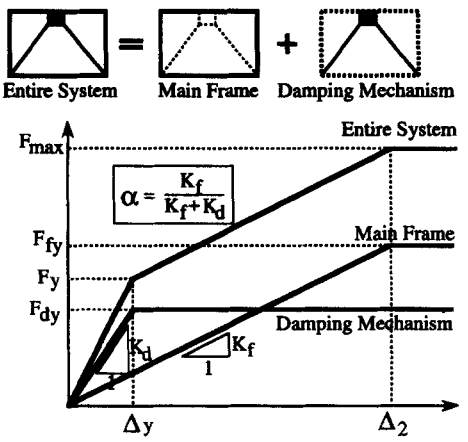

Figure 1. Schematic restoring force behaviour of structures with hysteretic dampers

dampers; a triangle-shaped version of ADAS devices,[4] called TADAS dampers; and shear panel dampers.[5] Lately, to enhance energy dissipation of these hysteretic dampers in even smaller vibrations and also to ensure initiation of energy dissipation at a strength prescribed in design, attempts have been made to use as the damper's material a high-quality, low-yield steel, for example, see Reference 6. The steel has a significantly smaller yield stress (80 MPa) and a larger rupture strain (40–60 per cent) than conventional mild steels, and the scatter of the yield stress from the nominal value is also maintained small.

The resistance behaviour of a structural system with a hysteretic damper can be simplified as in Figure 1. In this figure, the system consists of a main frame (serving primarily as the gravity force carrying system) and a hysteretic damping mechanism, with the two components being linked in parallel. The first yielding of the system corresponds to the yielding of the damping mechanism, while the second significant change in stiffness occurs at yielding of the main frame. The ratio of the stiffness after the first yielding (called the second stiffness) relative to the initial elastic stiffness (called the initial stiffness) is a function of the relative stiffness between the main frame and damping mechanism. In this paper, this ratio is named the ratio of second stiffness and designated as α. With reference to Figure 1, a design strategy for maximizing the benefit of hysteretic damping would be as follows: (1) to set the first yielding (F_y, Δ_y), i.e., yielding of the damping mechanism, low for the purpose of triggering energy dissipation as early as possible and (2) to set the maximum resistance (F_{max}), i.e. yielding of the main frame, large for the purpose of retarding serious structural damage to the main frame as much as possible. According to previous designs applied for structures with hysteretic dampers, the ratio of second stiffness [$\alpha = K_f/(K_f + K_d)$ in Figure 1] cannot be assigned a small value, i.e., the main frame cannot be designed so flexibly as compared to the hysteretic damping mechanism because of the lateral stiffness provided to the frame in the course of design for design vertical load and others, and the ratio of second stiffness easily reaches more than 0·5. [6,7]

The idea of energy-based seismic design was first advocated in a paper by Housner[8] and examined successively by many researchers in the world, for example see References 9–18. Particularly notable among those is Akiyama, whose extensive investigation (summarized in Reference 13) formed the basis of some Japanese seismic design guidelines. [19,20]As stated above, structures with hysteretic dampers rely for their seismic safety on the energy dissipation provided by the dampers, and thus their energy dissipation capacity and demand are of critical concern in seismic design. Considering its capacity to deal explicitly with both the energy dissipation capacity and the energy dissipation demand, the energy-based seismic design method is a very logical choice for the design of such structures.

Two key quantities in the energy-based seismic design are the total energy exerted on the system, E_t, and the hysteretic energy dissipated during the ground motion, E_p. These terms are commonly expressed in terms of equivalent velocities V_t and V_p, defined, respectively, as

$$E_t = \tfrac{1}{2}MV_t^2 \tag{1}$$

$$E_p = \tfrac{1}{2}MV_p^2 \tag{2}$$

where M is the mass of the system. According to previous investigations, both V_t and V_p are relatively constant with respect to the natural period of the system, T, except for the short range of T, and V_t and V_p remain relatively unchanged regardless of the yield strength in the inelastic system. It is notable that a majority of previous investigations used the linearly elastic and perfectly plastic model or the bilinear model with small ratios of second stiffness, for example, 5 per cent in Reference 11, 10 per cent in Reference 18, and at most 25 per cent in Reference 16, and from these investigations, it has been claimed that the effect of second stiffness on the energy behaviour is not major. As discussed earlier, however, the ratio of second stiffness could be much larger than those values examined previously. Thus, whether or not the major findings on the energy behaviour are still applicable for systems with large ratios of second stiffness is something that needs confirmation before energy-based seismic design for structures with hysteretic dampers is adopted.

This paper presents behavioural observations on the effects of rather large ratios of second stiffness characteristic of such structures on major parameters involved in energy-based seismic design. Specific subjects of investigation are (1) the effect of the ratio of second stiffness on the total input and hysteretic energies and (2) the effect of the ratio of second stiffness on the distribution of the hysteretic energy over the stories of multi-storey buildings.

ANALYSIS

Assumptions and analysis methods

Similar to many previous studies, the writers resorted to parametric numerical analysis using the direct integration method for obtaining necessary data. The restoring force behaviour was modelled as bilinear (Figure 2), in which the elastic stiffness and the stiffness in the second branch are $K_t(= K_f + K_d)$ and αK_t, respectively. As shown in Figure 1, the real restoring force behaviour is rather trilinear, but in the analysis it was decided to stick to the bilinear model because, using this model, we could directly evaluate the maximum resistance, F_{max}, and corresponding deflection, Δ_2, that would be required for the structure not to experience the third branch. As explained earlier, the third branch represents the state where the main frame exhibits inelastic excursions, and this is a state that should be avoided as much as possible.

The following three ground acceleration records were used for the analysis: the 1940 El Centro earthquake record (N–S component), the 1952 Taft earthquake record (N–S component), and the 1978 Miyagiken-oki

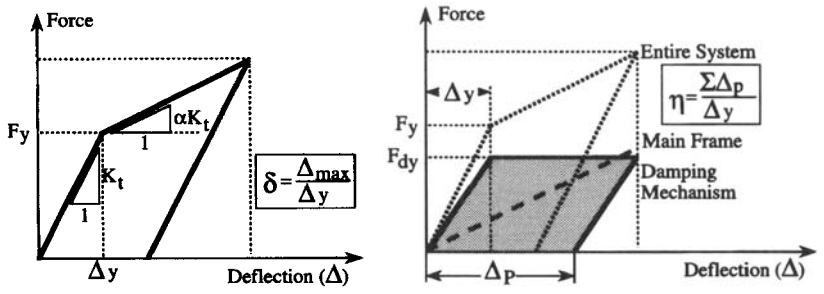

(a) Bilinear Hysteresis Model (b) Definition of Plastic Deformation

Figure 2. Bilinear system adopted and definition of major quantities

earthquake record (N–S component). All of these three earthquake records fall into the category of far-field motions having a long duration and cyclic excitations of a symmetric type. (Note that dampers are known to be most effective for this type of ground motion.) The variables selected in the analysis were (1) the natural period of the system, calculated with respect to the initial elastic stiffness, K_t (T = 0·15–4·0 sec), (2) the viscous damping ratio (h = 0·0, 0·02, 0·05, or 0·1 of critical), (3) the ratio of second stiffness (α = 0, 0·1, 0·25, 0·5, or 0·75), and (4) the yield strength, F_y. The yield strength of the system was selected in two ways. In one case, the yield strength was assigned as a fraction of the maximum force exerted on the structure F_e, if the structure responded only elastically, and 0·125, 0·25, and 0·5 were adopted for F_y/F_e. In the other case, the yield strength was adjusted so that the maximum ductility ratio, δ: the maximum deflection experienced during the motion, Δ_{max}, divided by the yield deflection, Δ_y, would be 3, 5, or 7.

Behaviour of total input energy and hysteretic energy

Figure 3 shows the V_t spectra with respect to the viscous damping ratio (h = 0·02, 0·05, and 0·1). Figures 3(a) and 3(c) (those on the left side of Figure 3) show the V_t spectra for a small second stiffness (α = 0·1). It should be pointed out that the differences observed among the three viscous damping ratios are those that have been considered minor by previous investigators, and that judgment, although somewhat subjective, forms the basis for the contention that the total input energy remains relatively constant regardless of the magnitude of viscous damping. Figures 3(b) and 3(d) (those on the right side of Figure 3) show the V_t spectra for α = 0·75, indicating that the differences among the viscous damping ratios are commensurate overall with those observed for α = 0·1.

Figure 4 shows the V_t spectra with respect to the maximum ductility ratios (δ = 3, 5, and 7). Figures 4(a) and 4(c) are given for α = 0·1, indicating that the degree of variation resulting from the choice of δ is slightly larger than that observed with respect to h, but this level of variation has still been considered to be secondary by previous investigators, who claim that the total input energy is relatively unaffected with respect to the maximum ductility (or equivalently the yield strength). Figures 4(b) and 4(d), given for α = 0·75, show that, with respect to δ, V_t is less sensitive for α = 0·75 than for α = 0·1, which can be interpreted with reference to a simple examination shown in Figure 5. Provided one cycle with a given ductility of 3, 5, and 7, the secant stiffness (the slope of the line connecting the two extreme displacements) relative to the initial elastic stiffness is 1/3 (δ = 3), 1/5 (δ = 5), and 1/7 (δ = 7) where α = 0·0, whereas the ratio is 2/3 (δ = 3), 3/5

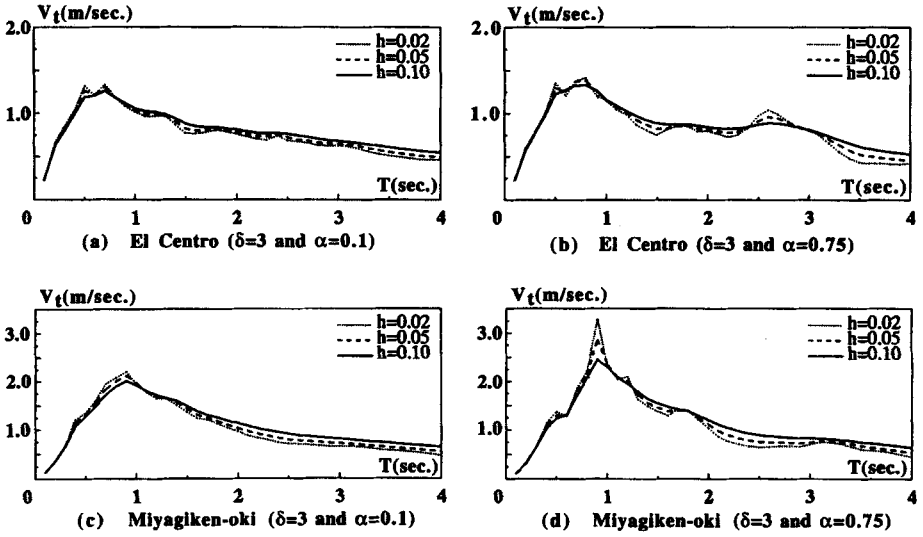

Figure 3. Effect of viscous damping on total input energy (h, viscous damping ratio)

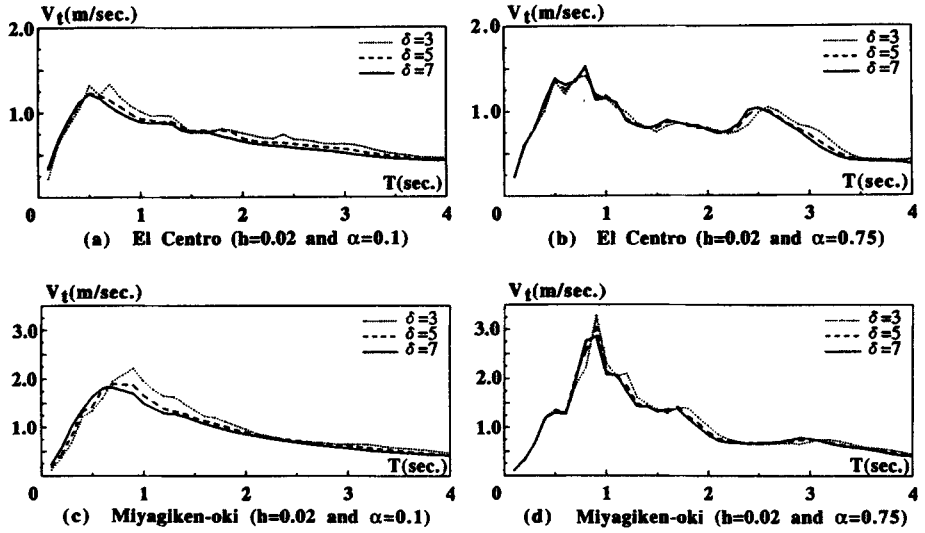

Figure 4. Effect of maximum ductility on total input energy

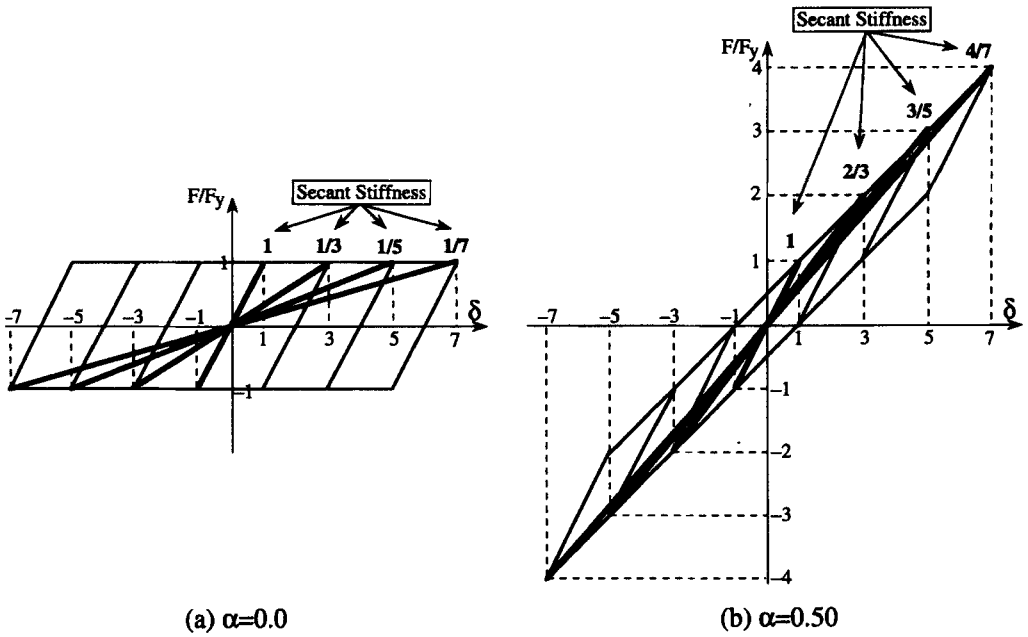

Figure 5. Stiffness shift in non-linear response

($\delta = 5$), and 4/7 ($\delta = 7$) when $\alpha = 0{\cdot}5$. This indicates that stiffness reduction (meaning elongation of the apparent natural period) by the increase of δ is more conspicuous when α is smaller. Since a larger shift in the vibration period is a source of a larger change of the response, it is conceivable that the effect of δ on the total input energy is less significant with the increase of α.

Figure 6 shows the effects of the ratio of second stiffness, α, on the total input energy, V_t, indicating that V_t is reasonably unchanged regardless of the value of α. In a narrow range of natural periods where the maximum value of V_t is obtained, V_t tends to increase for larger α's. This trend is understandable, because the

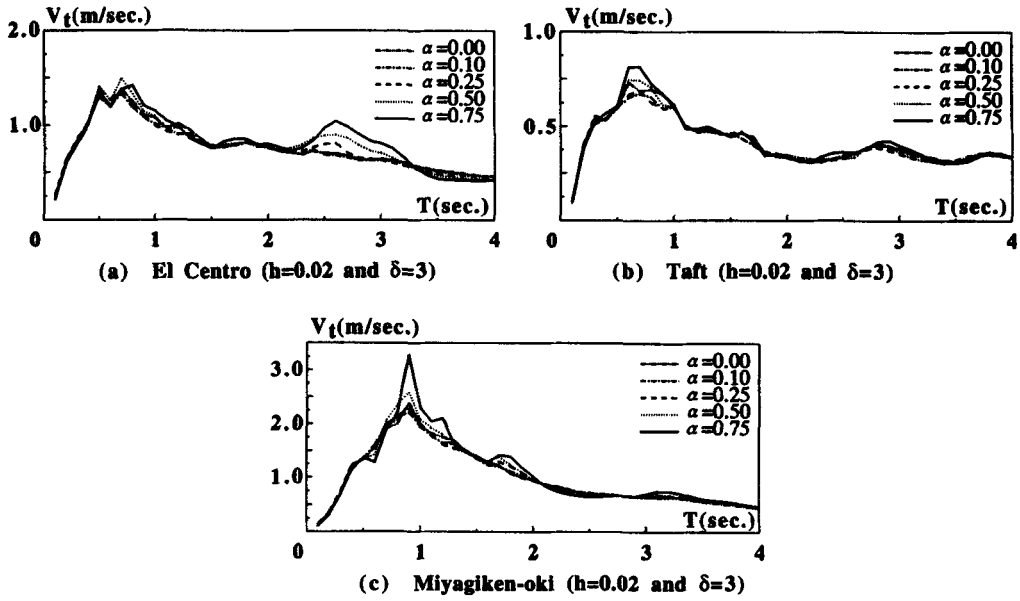

Figure 6. Effect of ratio of second stiffness on total input energy

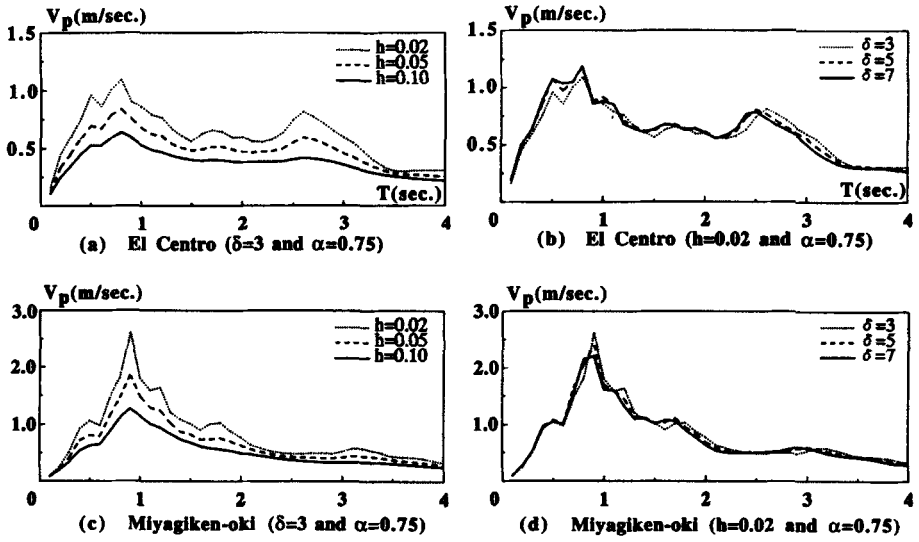

Figure 7. Effect of viscous damping and maximum ductility on hysteretic energy

larger the value of α is, the more the system behaves like the elastic system, while the fluctuation of V_t spectra as well as the increase in response at the resonant period are known to be more significant in the elastic system than in the inelastic system, particularly when the system is lightly damped. To summarize, the effect of the ratio of second stiffness, α, on V_t is judged to be not major, because change in V_t is at most 35 per cent [Figure 6(c)] and confined only in a small range of period.

Figure 7 shows the hysteretic energy spectra (in terms of V_p) of systems with $\alpha = 0{\cdot}75$ for two earthquake records, various viscous damping ratios and maximum ductility ratios. Viscous damping affects V_p a great deal [Figures 7(a) and 7(c)]; a larger viscous damping ratio gives a smaller V_p. This observation is the same as

Table I. Ratios of hysteretic energy to total input energy

	$V_p V_t$					
	$h = 0{\cdot}02$			$h = 0{\cdot}05$		
α	El Centro	Taft	Miyagikenoki	El Centro	Taft	Miyagikenoki
0·0	0·861	0·881	0·896	0·783	0·771	0·792
0·10	0·854	0·890	0·912	0·765	0·758	0·778
0·25	0·869	0·860	0·878	0·728	0·741	0·750
0·50	0·835	0·853	0·857	0·657	0·679	0·723
0·75	0·753	0·781	0·796	0·586	0·598	0·635

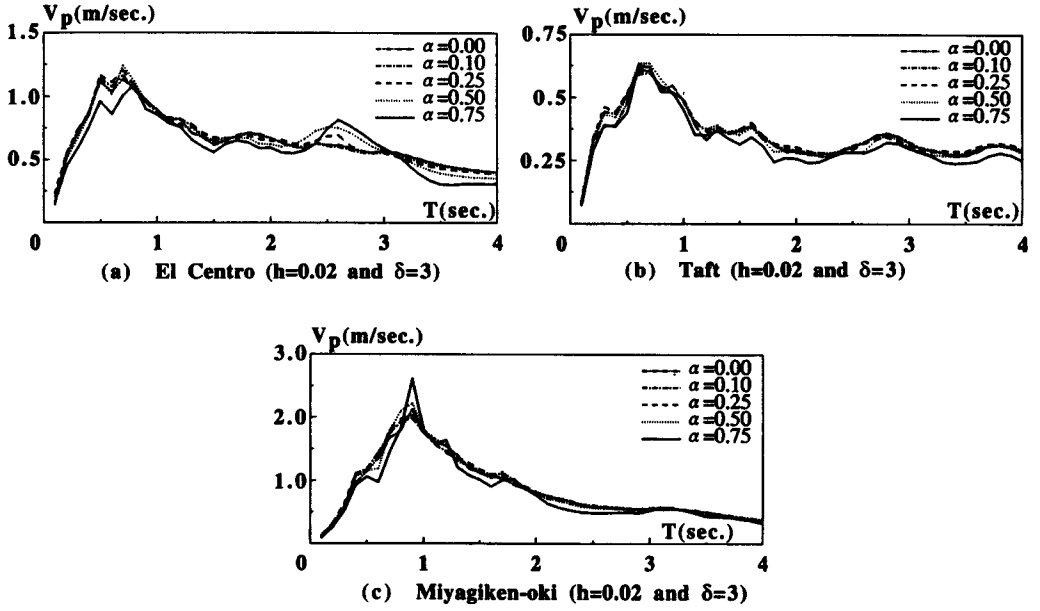

Figure 8. Effect of ratio of second stiffness on hysteretic energy

that derived from earlier studies. The ratios of V_p to V_t (values averaged over the natural period) are summarized in Table I.

On the other hand, comparison of Figures 7(b) and 7(d) and Figures 4(b) and 4(d) indicates that the maximum ductility (or, equivalently, the yield strength) affects the hysteretic energy as little as the total input energy. According to Figure 8, which shows the effect of the ratio of second stiffness, α, on the hysteretic energy, V_p, V_p changes also as little as V_t (shown in Figure 6) for different α's. These observations support that the hysteretic energy remains relatively unchanged with respect to the maximum ductility and the ratio of second stiffness. If anything, the V_p spectrum is made somewhat smaller with the increase of α (Figure 8). This observation is confirmed in Table I, which shows that the increase of α reduces the ratio of V_p to V_t; for example, 0·86-0·90 ($\alpha = 0{\cdot}0$) down to 0·75–0·80 ($\alpha = 0{\cdot}75$) for $h = 0{\cdot}02$ and 0·77–0·80 ($\alpha = 0{\cdot}0$) down to 0·59–0·64 ($\alpha = 0{\cdot}75$) for $h = 0{\cdot}05$, respectively. Such reduction is understandable because, with the increase in α, the system behaves more elastically and more energy is dissipated by viscous damping, which results in relative reduction of the hysteretic energy.

Interrelation between hysteresis energy, cumulative plastic deformation, and maximum ductility

The hysteretic energy can be converted to another quantity called the cumulative plastic deformation. In the hysteresis shown in Figure 2(b), the plastic deformation of the damper, Δ_p, is defined as the distance between two adjacent unloaded deflections, i.e. from the beginning to the end of one half cycle of hysteresis. The sum of the plastic deformations over the response is the cumulative plastic deformation $\Sigma\Delta_p$, and its ratio to the yield deformation, Δ_y, is designated as the ratio of cumulative plastic deformation, η. Since the hysteretic energy dissipated by the system equals the total area enclosed by the hysteresis curves, the ratio of cumulative plastic deformation, η, and the hysteretic energy, E_p, are related as

$$\eta = \frac{E_p}{(1-\alpha)F_y\Delta_y} \tag{3}$$

where $(1-\alpha)F_y$ equals the damper's yield strength, F_{dy}.

As stated earlier, the maximum deformation expected during the response is also a very critical parameter that should not be overlooked in design. This statement is justified, because the knowledge of δ makes it possible to estimate F_{max} and Δ_2 (Figure 1) that would be required for the main frame to survive without damage. Based upon the numerical data accumulated in this study, the following empirical expression was obtained for the ratio of the maximum ductility, δ, to the corresponding ratio of cumulative plastic deformation, η, as

$$\frac{\delta-1}{\eta} = \frac{1}{\delta+1} \tag{4}$$

[Here $(\delta-1)$ is used instead of δ for the maximum ductility term, because δ includes the effect of elastic limit deformation, Δ_y.] Equation (4) is rewritten as

$$\delta = \sqrt{\eta+1} \tag{5}$$

Figure 9 shows examples of relationships between the numerically obtained maximum ductility ratio, δ, and the maximum ductility ratio estimated using equations (3) and (5), designated as δ' in the figures,

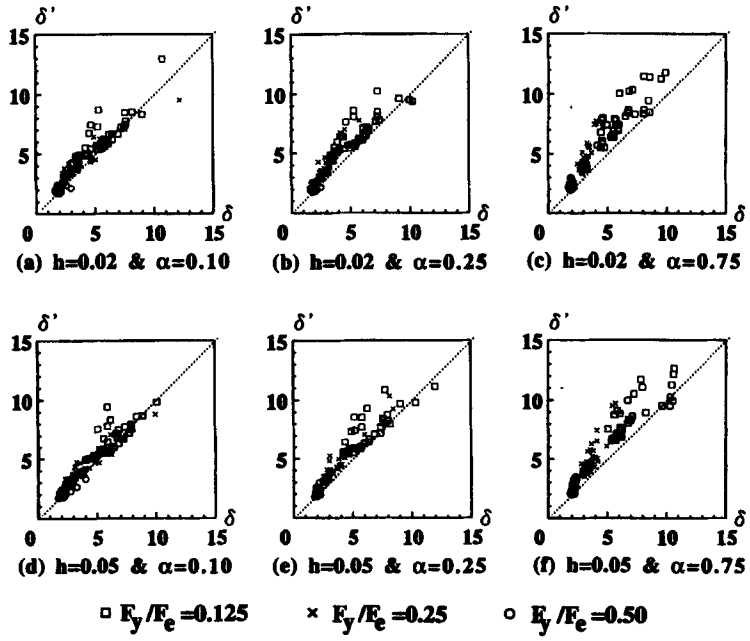

Figure 9. Correlation between numerical maximum ductility ratio, δ, and estimated maximum ductility ratio, δ' (El Centro Earthquake Record)

Table II Relationship between yield strength and maximum deformation

α	F_y/F_e	V_t (m/sec)	V_p (m/sec)	Δ_y (mm)	δ	η	$\delta\Delta_y$ (mm)	$\eta\Delta_y$ (mm)
	0·10	0·912	0·814	16·8	5·42	29·7	91·2	499
	0·15	0·985	0·852	25·2	3·36	14·5	84·9	365
	0·20	1·06	0·894	33·7	2·77	8·94	93·1	301
0·1	0·30	1·10	0·873	50·5	1·86	3·78	93·9	191
	0·40	1·11	0·844	67·3	1·60	1·99	108	134
	0·60	1·12	0·776	101	1·38	0·741	139	74·9
	0·10	1·15	0·874	16·8	6·77	34·2	114	575
	0·15	1·19	0·912	25·2	4·48	16·6	113	418
	0·20	1·17	0·883	33·7	3·34	8·72	112	293
0·75	0·30	1·11	0·788	50·5	2·34	3·09	118	156
	0·40	1·10	0·763	67·3	1·89	1·62	127	109
	0·60	1·10	0·680	101	1·45	0·573	146	57·9

demonstrating that correlation between the true and estimated maximum ductility ratios is reasonable. [Note that equation (4) was established considering the conservatism required for ensuring structural safety, and, as a result, a majority of the data are plotted on the conservative side.] Equation (5) was derived empirically based only upon the data accumulated in the study presented and therefore is considered yet to be rudimentary. Nevertheless, the writers wish to present it, with the recognition that practical information on the relationship between δ and η is very critical in design but not widely available at the present time.

Design consideration for systems with hysteretic dampers

Based upon the examinations presented, the premise of the energy-based seismic design was found to be applicable also for systems having a large ratio of second stiffness, α; that is, both the V_t and V_p spectra are relatively insensitive to the yield strength and/or α (as much as 0·75 in this study). In the seismic design of a structure with a hysteretic damper, if a design V_p spectrum is assigned, the ratio of cumulative plastic deformation demanded of the hysteretic damper is estimated from equations (2) and (3). Safety of the structure will then be assured by designing the damper such that its capacity for the ratio of cumulative plastic deformation be not smaller than the demanded ratio of cumulative plastic deformation. Further, equation (5) gives the expected maximum ductility ratio, from which one can check whether or not the main frame can remain elastic or alternatively can design the main frame so that it would be strong enough not to exhibit yielding and inelastic excursions.

In the design consideration, the relationship between the yield strength and maximum deformation is worth noting. Table II lists values of V_t, V_p, Δ_y (the yield deformation), δ (the maximum ductility ratio), η (the ratio of cumulative plastic deformation), $\delta\Delta_y$ (the maximum deformation), and $\eta\Delta_y$ (the cumulative plastic deformation) for various yield strengths ($F_y/F_e = 0{\cdot}1$–$0{\cdot}6$). The data were obtained for a system having $T = 1{\cdot}0$ sec, h (the viscous damping ratio) = 0·02, and $\alpha = 0{\cdot}1$ and 0·75 and subjected to the 1940 El Centro earthquake record. When the yield strength is small ($F_y/F_e < 0{\cdot}3$), the maximum deformation, $\delta\Delta_y$, is relatively constant, but it increases for larger yield strength values. This behaviour can also be supported by equations (2), (3), and (5) as follows. If the yield strength is increased twice with the elastic stiffness being unchanged, the yield deformation, Δ_y, also is enlarged twice [Figure 2(b)], whereas the required ratio of cumulative plastic deformation, η, is reduced to one-quarter because of equation (3) with the assumption that E_p is constant. According to equation (5), the reduction of η to one-quarter leads the maximum ductility ratio, δ, to more than one-half [because of the unity added to η in the square root of equation (5)], resulting that the maximum deformation, given as the product of δ (more than one-half) and Δ_y (exactly twice), becomes larger for the system in which the yield strength is increased twice. [Note that, if $\delta = \sqrt{\eta}$ were used instead of equation (5), δ would be exactly one-half, and the maximum deformation would remain the same.]

Furthermore, it is notable that the rate of increase in the maximum deformation due to the increase of the yield strength is smaller for smaller yield strengths, because a smaller yield strength makes η larger and the effect of the unity appearing in the square root of equation (5) vanishes.

This observation indicates that, for a system having a stronger hysteretic damper, a larger yield deformation and strength is required for the main frame to survive without damage. For this reason as well as for the reason to ensure an early onset of energy dissipation, it is advisable to keep the yield strength of hysteretic dampers low, while designing the dampers to possess sufficient cumulative plastic deformation capacity. Hysteretic dampers made of a high-quality, low yield steel have been developed to comply with this need.

ENERGY BEHAVIOUR OF MDOF SYSTEMS

Analysis of MDOF systems

According to previous studies,[10,13] the energy behaviour of multi-storey buildings is summarized such that both the total input and hysteretic energies of a multi-storey building, represented as an MDOF system, are primarily a function of the total mass, M_T, and the fundamental natural period, T_1, and approximately equal the total input and hysteretic energies exerted on an equivalent SDOF system having a mass of M_T and a natural period of T_1.

Assumptions imposed for selecting the vibrational properties of the analyzsed systems are as follows: (1) the system was represented by a spring–mass system, with the mass assumed to concentrate on each floor level and the storey shear versus storey deflection relationship taken to be bilinear; (2) the mass and storey height were the same for all stories, and a unit mass and a height of 4 m were assigned; (3) the yield strength was distributed over the stories so that all stories would yield simultaneously under the static design earthquake force profile specified in the Japanese Seismic Design Code; [21](4) distribution of the initial elastic stiffness over the stories was determined so that all stories would undergo the same yield deflection under the specified static design earthquake force; (5) the yield strength of the first storey F_{y1}, was determined so that the base shear coefficient at yielding would be 0·1; and (6) the yield deformation of 1/800 in terms of the storey drift angle was adopted, with the value chosen in reference to hysteretic dampers previously designed and analysed. [6,7]Assumptions adopted here conform approximately to those used in real structural design, although the base shear coefficient of 0·1 was somewhat smaller than the base shear coefficients adopted in various seismic design specifications. The value of 0·1 was chosen intentionally on the premise that, in a structure with hysteretic dampers, the force that triggers the dampers (meaning the yield force of the structure) would be set rather low in order to maximize the benefit of these dampers. Parameters used in the analysis were the same as those used in the analysis for SDOF systems. In addition, the number of stories, N was selected as one of 5, 10, 13, 15, 17, and 20.

Total input energy and hysteretic energy of MDOF systems

Figure 10 shows examples of the total input energy (in terms of V_i) and total hysteretic energy (in terms of V_p) obtained from the analysis, together with the spectra derived from the corresponding SDOF systems having the same natural period, damping ratio, and yield strength ($F_y/F_e = 0{\cdot}1$). The figure clearly shows that both V_i and V_p of an MDOF system are very close to those of the corresponding SDOF system, indicating that the key findings regarding the energy behaviour of MDOF systems hold true even if the ratio of the second stiffness, α, is large (as much as 0·75 in this study).

Distribution of hysteretic energy into stories

The total hysteretic energy dissipated by the system, E_{Tp}, is the sum of the hysteretic energies dissipated by respective stories. Thus,

$$E_{Tp} = \sum_{i=1}^{N} (1-\alpha) F_{y_i} \Delta y_i \eta_i \tag{6}$$

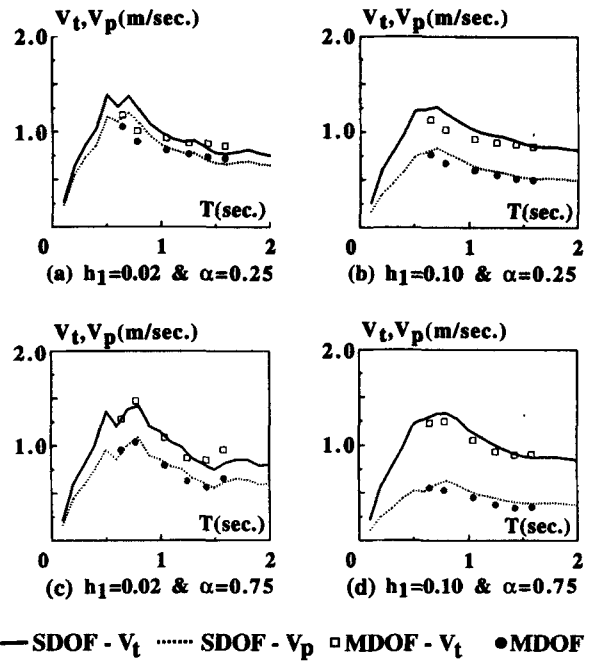

Figure 10. Comparison of total input energy and hysteretic energy between SDOF and MDOF systems (h', viscous damping ratio with respect to the first mode of elastic vibration)

where F_{yi}, Δ_{yi} and η_i are the yield strength, yield deflection and ratio of cumulative plastic deformation of the ith storey, respectively. Since the yield strength was distributed along the storey so that all stories would yield simultaneously under the static design earthquake force, it was hoped that the ratios of cumulative plastic deformation, η_i, were relatively constant throughout the stories, which means uniform damage of hysteretic dampers along the storey. If the ratio of cumulative plastic deformation is assumed to be constant, its ratio is estimated as

$$\eta = \frac{E_{Tp}}{\sum_{i=1}^{N}(1-\alpha)F_{yi}\Delta_{yi}} \tag{7}$$

Figure 11 shows the ratios of plastic deformation achieved in respective stories divided by η' for the 10- and 20-storey building models, indicaing that, when $\alpha = 0{\cdot}75$, the ratio of plastic deformation is distributed very uniformly except for the top storey, where the ratio is somewhat smaller. On the other hand, the ratio changes drastically along the stories when $\alpha = 0{\cdot}1$, and is larger for lower stories.

Here, a question arises as to how sensitive the distribution of the hysteretic energy would be with respect to the choice of the initial stiffness distribution and the yield strength distribution over the stories. From the design viewpoint, a large fluctuation of the hysteretic energy distribution caused by a small change in the stiffness and/or yield strength distribution is certainly undesirable, because fine adjustment of storey stiffnesses and yield strengths is not necessarily practical in design. In order to study the effects of distributions of the storey stiffness and yield strength on the distribution of the total hysteretic energy, additional analysis was carried out. Figure 12 shows the ratios of cumulative plastic deformation if one of the stories had a smaller yield strength (80 per cent of the yield strength assigned in the original analysis), with all other properties remaining unchanged. When $\alpha = 0{\cdot}1$, a large ratio of cumulative plastic deformation, meaning concentration of the hysteretic energy, is observed for the intentionally weakened storey (the first, fifth, and ninth stories for Figures 12(a), 12(b), and 12(c), respectively), but, when $\alpha = 0{\cdot}75$, distribution of the total hysteretic energy still remains uniform. Figure 12(d) shows the ratios of cumulative plastic deformation

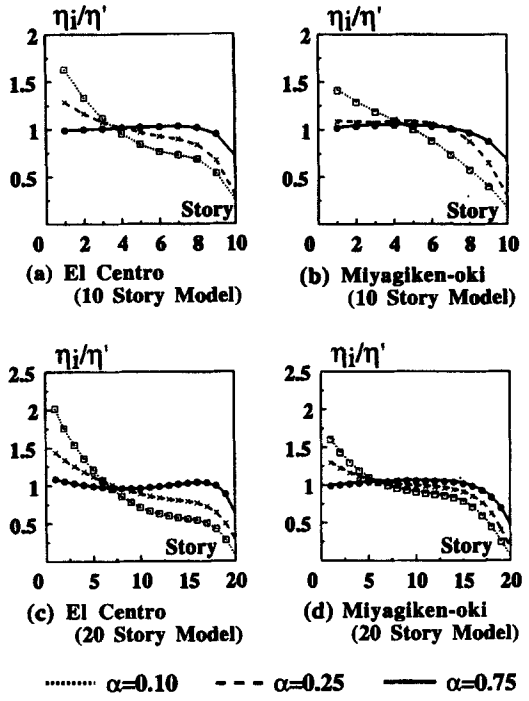

Figure 11. Distribution of hysteretic energy along storey

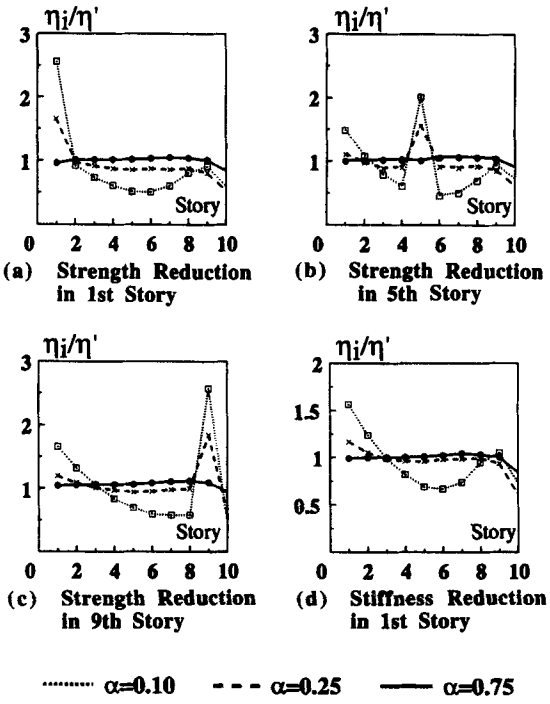

Figure 12. Effect of distribution of yield strength and stiffness on hysteretic energy distribution

when the first storey has a stiffness, that is 80 per cent of the original stiffness, with all other properties remaining the same. Comparison between Figure 11(a) (for the original system) and Figure 12(d) (for the system with the reduced stiffness) clearly demonstrates that when $\alpha = 0{\cdot}10$, the change in stiffness significantly alters the whole distribution of the total hysteretic energy, whereas when $\alpha = 0{\cdot}75$, the distribution remains nearly unchanged. These observations deliver an important message about the role of the second stiffness in the earthquake response behaviour of multi-storey buildings. That is, with a good amount of second stiffness (say $\alpha = 0{\cdot}75$), uniform distribution of the hysteretic energy can be achieved easily, and robustness in the hysteretic energy distribution against unavoidable fluctuations of the storey stiffness and yield strength is also assured. With reference to Figure 1, this observation suggests the importance of supplying a good amount of stiffness to the main frame to ensure a uniform distribution of the hysteretic energy to individual hysteretic dampers.

CONCLUSION

This paper presented qualitative observations on the energy behaviour of structures having hysteretic dampers, which are characterized by a large ratio of the second stiffness (after yielding) to the initial elastic stiffness, α. A summary of this study is as follows:

(1) The total input energy and hysteretic energy become less insensitive to the yield strength (or, equivalently, to the maximum ductility) with the increase of α (as much as 0·75 in this study). With the increase of α, the total input energy tends to increase, but the increase is confined only around the natural period where the total input energy takes the maximum value.
(2) A simple empirical formula that correlates the ratio of cumulative plastic deformation to the maximum ductility ratio was proposed.
(3) Even when α is large, the total input energy and hysteretic energy for MDOF systems are approximately the same as those of an equivalent SDOF system that has the same mass, natural period, yield strength and α.
(4) Effects of α on the distribution of the hysteretic energy over the stories were examined, and it was found that a good amount of α is very effective for distributing the energy uniformly.

REFERENCES

1. R. D. Hanson, I. D. Aiken, D. K. Nims, P. J. Richter and R. E. Bachman, 'State-of-the-art and state-of-the-practice in seismic energy dissipation', *Proc. seminar on seismic isolation, passive energy dissipation, and active control*, Vol. 2, Applied Technology Council, 1993, pp. 449–471.
2. I. D. Aiken, K. D. K. Nims, A. S. Whittaker and J. M. Kelly, 'Testing of passive energy dissipation systems', *Earthquake spectra* **9**, 335–370 (1993).
3. S. F. Stiemer, W. G. Godden and J. M. Kelly, 'Experimental behavior of a spatial piping system with steel energy absorbers subjected to a simulated differential seismic input', *Report No. UCB/EERC-81/09*, Earthquake Engineering Research Center, 1981.
4. K. C. Tsai and C. P. Hong, 'Steel triangular plate energy absorber for earthquake-resistant buildings', *Proc. 1st world conf. on constructional steel design*, Acapulco, Mexico, 1992, pp. 345–355.
5. H. Tamai, H. Takenaka, A. Kunisue, K. Kondo and M. Hanai, 'On hysteretic damper using low yield stress steel plate installed in K-braced frame, Part 1 and 2', *Proc. annual meeting of the architectural inst. of Japan*, Tokyo, Japan, 1991, pp. 1447–1450 (in Japanese).
6. M. Nakashima, S. Iwai, M. Iwata, T. Takeuchi, S. Konomi, K. Saburi and T. Akazawa, 'Energy dissipation behavior of shear panels made of low yield steel', *Earthquake eng. struct. dyn.* **23**, 1299–1313 (1994).
7. K. C. Tsai, H. W. Chen, C. P. Hong and Y. F. Su, 'Design of steel triangular plate energy absorbers for seismic-resistance construction', *Earthquake spectra* **9**, 505–528 (1993).
8. G. W. Housner, 'Limit design of structures to resist earthquakes', *Proc. 1st world conf. on earthquake engineering*, Berkeley, CA, 1956, pp. 5.1–5.13.
9. B. Kato and H. Akiyama, 'Energy input and damages in structures subject to severe earthquakes', *Trans. architect. inst. Japan* (235) 9–18 (1975) (in Japanese).
10. W. E. McKevitt, D. L. Anderson, N. D. Nathan and S. Cherry, 'Towards a simple energy method for seismic design of structures', *Proc. 2nd U.S. national conf. on earthquake engineering*, 1979, pp. 383–392.
11. T. F. Zahrah and W. J. Hall, 'Seismic energy absorption in simple structures', in *Civil Engineering Studies*, Structural Research Series No. 501, University of Illinois, Urbana, IL, 1982.
12. T. Zahrah and W. J. Hall, 'Earthquake energy absorption in SDOF structures', *J. struct. eng. ASCE* **110**, 1757–1772 (1984).

13. H. Akiyama, *Earthquake-Resistant Limit-State Design of Building*, University of Tokyo Press, Tokyo, 1985.
14. S. L. McCabe and W. J. Hall, 'Assessment of seismic structural damage', *J. struct. eng. ASCE* **115**, 2166–2183 (1989).
15. C. M. Uang and V. V. Bertero, 'Evaluation of seismic energy in structures', *Earthquake eng. struct. dyn.* **19**, 77–90 (1990).
16. P. Leger and S. Dussault, 'Seismic-energy dissipation in MDOF structures', *J. struct. eng. ASCE* **118**, 1251–1269 (1992).
17. P. Fajfar, 'Equivalent ductility factors, taking into account low-cycle fatigue', *Earthquake eng. struct. dyn.* **21**, 837–848 (1992).
18. M. Rodriguez, 'A measure of the capacity of earthquake ground motions to damage structures', *Earthquake eng. struct. dyn.* **21**, 627–643 (1992).
19. 'Ultimate strength and deformation capacity of buildings in seismic design', The Architectural Institute of Japan, 1981 (in Japanese).
20. 'Recommendation for the design of based isolated buildings', The Architectural Institute of Japan, 1989 (in Japanese).
21. 'Guide and commentary for structural design', The Building Center of Japan, 1981 (in Japanese).